High temperature elastic anisotropy of the perovskite and post-perovskite polymorphs of Al_2O_3

Stephen Stackhouse, John P. Brodholt, and G. David Price

Department of Earth Sciences, University College London, London, UK

[1] Finite temperature ab initio molecular dynamics calculations were performed to determine the high temperature elastic and seismic properties of the perovskite and post-perovskite phases of pure end-member Al_2O_3. The post-perovskite phase exhibits very large degrees of shear-wave splitting. The incorporation of a few mole percent of Al_2O_3 into $MgSiO_3$ is predicted to have little effect on the perovskite to post-perovskite phase transition pressure and seismic properties of the post-perovskite phase; although a small difference in shear-wave splitting may be observable. **Citation:** Stackhouse, S., J. P. Brodholt, and G. D. Price (2005), High temperature elastic anisotropy of the perovskite and post-perovskite polymorphs of Al_2O_3, *Geophys. Res. Lett.*, *32*, L13305, doi:10.1029/2005GL023163.

1. Introduction

[2] The recently reported post-perovskite phase transition in pure end-member $MgSiO_3$ [*Murakami et al.*, 2004; *Shim et al.*, 2004] provides a potential explanation for the seismic discontinuity seen atop of the D'' layer [*Sidorin et al.*, 1999] and implicates post-perovskite as the dominant phase in the lowermost mantle. Further evidence for this comes from theoretical calculations [*Oganov and Ono*, 2004; *Iitaka et al.*, 2004; *Tsuchiya et al.*, 2004a, 2004b; *Stackhouse et al.*, 2005], which show that the phase could produce seismic anisotropy consistent with that observed at the base of the lower mantle [*Kendall and Silver*, 1998; *Panning and Romanowicz*, 2004] and also the expected anti-correlation of bulk and shear velocities [*Su and Dziewonski*, 1997]. Studies of the phase transition have, however, in general, been limited to its occurrence in pure end-member $MgSiO_3$ and neglected the effect of minor elements thought to be incorporated into perovskite in the mantle [*Irifune*, 1994; *Wood and Rubie*, 1996]. One exception is the high-pressure experiments of [*Mao et al.*, 2004], who synthesized a ferromagnesian post-perovskite phase and demonstrated that incorporation of iron greatly reduces the pressure required for the phase transition from perovskite to post-perovskite. In addition, theoretical investigations into the phase transition between the perovskite and post-perovskite polymorphs of pure end-member Al_2O_3 have also been reported [*Caracas and Cohen*, 2005]. These showed the incorporation of Al_2O_3 into $MgSiO_3$ raises the perovskite to post-perovskite phase transition pressure, relative to that for the pure $MgSiO_3$ end-members. In this paper we consider the high-temperature elastic properties of the perovskite and post-perovskite phases of pure end-member Al_2O_3 and their possible geophysical implications.

[3] There are two mechanisms by which aluminum may enter the pure end-member perovskite and post-perovskite polymorphs of $MgSiO_3$. The first, is the so called oxygen vacancy-forming mechanism, whereby two silicon atoms and one oxygen atom are replaced by two aluminum atoms, leaving an oxygen vacancy: $2Si^{4+} + O^{2-} \rightarrow 2Al^{3+}$. The second, known as the charge coupled substitution mechanism, involves the substitution of one magnesium atom and one silicon atom each by an aluminum atom: $Mg^{2+} + Si^{4+} \rightarrow 2Al^{3+}$. There is a consensus, however, that the dominant substitution mechanism in the deep lower mantle is the charge coupled substitution mechanism [*Brodholt*, 2000; *Yamamoto et al.*, 2003; *Akber-Knutson and Bukowinski*, 2004]. Even though most proposed mantle compositions [*Anderson*, 1989] suggest that perovskite and post-perovskite in the lower mantle can only incorporate up to four mole percent Al_2O_3, we can estimate the effect that this would have on their stabilities and elastic properties from investigation of the pure aluminum end-members, which are meta-stable phases under core-mantle boundary conditions [*Caracas and Cohen*, 2005].

2. Computational Details

[4] Calculations were performed in an identical manner to those in previous work [*Stackhouse et al.*, 2005], using the projector-augmented-wave (PAW) implementation [*Blöchl*, 1994; *Kresse and Joubert*, 1999] of the density functional theory based VASP code [*Kresse and Furthmüller*, 1996a, 1996b]. This utilizes a plane-wave basis set, periodic boundary conditions and **k**-point sampling. The exchange-correlation functional used adhered to the PW91 form of the generalized gradient approximation [*Wang and Perdew*, 1991; *Perdew et al.*, 1992].

[5] Models of the perovskite and post-perovskite polymorphs of pure end-member Al_2O_3 were constructed using coordinates calculated for the $MgSiO_3$ forms of the phases in previous studies [*Oganov et al.*, 2001; *Stackhouse et al.*, 2005]. In the first instance, 20 atom models of the perovskite and post-perovskite forms of pure end-member $MgSiO_3$ and Al_2O_3 were optimized at several pressures in the range 80–180 GPa, using a plane-wave cut-off of 800 eV and sampling the Brillouin zone using Monkhorst-Pack grids [*Monkhorst and Pack*, 1976] of $4 \times 4 \times 4$ for the perovskite phase and $6 \times 6 \times 4$ for the post-perovskite phase. To determine the athermal elastic constants of the Al_2O_3 systems at 136 GPa, three different orthorhombic and one triclinic type strains, of magnitude ±0.3, ±0.7 and ±1.0 percent were applied to the optimized equilibrium
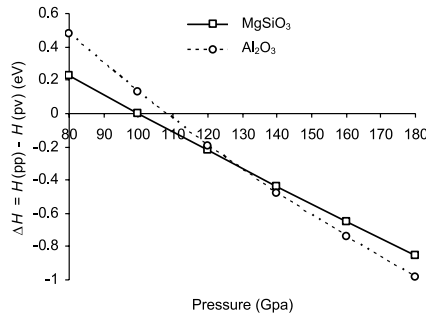
Figure 1. Enthalpy difference between the perovskite and post-perovskite polymorphs of MgSiO$_3$ and Al$_2$O$_3$ as a function of pressure.

models, the induced stresses calculated and the resultant stress-strain relation fit to a second-order polynomial to remove non-linear contributions. Increasing the plane-wave cut-off to 1000 eV and the Monkhorst-Pack grids by two **k**-points in each direction caused the calculated enthalpy difference of the two phases to change by less than 1.0 meV per atom and the absolute value of the elastic constants to differ by an average of 0.6 percent. The calculations were therefore considered converged.

[6] To determine finite temperature elastic constants a similar procedure was followed using high temperature molecular dynamics instead of athermal optimizations. For these simulations an 80 atom model of the perovskite phase and a 60 atom model of the post-perovskite phase were used. The time-step for the simulations was 1 fs. Since the VASP code dictates fixed volume calculations, the simulations were performed using a rigid cell. To obtain equilibrium structures at a simulated isotropic pressure of 136 GPa at a temperature of 4000 K, repeated simulations were run, adjusting the cell dimensions each time, until the average stress over 2 ps was within 0.5 GPa in each of the principal directions. The large size of the models and computational expense of ab initio molecular dynamics prescribed that Brillouin zone sampling was restricted to the Γ- point, the plane-wave cut-off reduced to 500 eV and induced stresses calculated as the average over 1 ps

simulation for strains of magnitude ±1.0 percent only. Note that, athermal elastic constants calculated using the larger models and reduced basis-set criteria differed by an average of only 1.4 percent from those determined using the 20 atom models and larger basis-set.

[7] Single-crystal compressional and shear-wave velocities were calculated from their corresponding elastic constants by solving the Christoffel matrix [*Musgrave*, 1970]. Single crystal elasticities were converted to transversely isotropic symmetries using the method outlined by [*Wentzcovitch et al.*, 1998].

3. Results and Discussion

[8] The difference in enthalpy of the perovskite and post-perovskite polymorphs of MgSiO$_3$ and Al$_2$O$_3$, over the pressure range 80–180 GPa, is presented in Figure 1. The calculated perovskite to post-perovskite transition pressure (neglecting temperature) is about 100 GPa for MgSiO$_3$, in agreement with previous theoretical studies [*Oganov and Ono*, 2004; *Iitaka et al.*, 2004], but lower than the 125 GPa determined from experimental work [*Murakami et al.*, 2004]. This is because the calculations neglect thermal effects. High-temperature calculations within the quasi harmonic approximation showed that the phase transition pressure increases by about 30 GPa when determined at 4000 K as opposed to 0 K [*Tsuchiya et al.*, 2004a].

[9] The calculated perovskite to post-perovskite phase transition pressure for pure end-member Al$_2$O$_3$ is about 110 GPa, which is only 10 GPa higher than that of pure end-member MgSiO$_3$. Most proposed mantle compositions contain an average of four mole percent Al$_2$O$_3$ [*Anderson*, 1989]. If we assume simple linear mixing, our calculations suggest that incorporation of this percentage of Al$_2$O$_3$ into MgSiO$_3$ would increase the post-perovskite phase-transition, on the order of 0.5 GPa, which agrees well with the 1 GPa, proposed by [*Caracas and Cohen*, 2005].

[10] Elastic constants calculated for the perovskite and post-perovskite phases of Al$_2$O$_3$ are listed in Table 1, with corresponding unit cell parameters, volumes and densities given in Table 2. The compressional and shear-wave velocities determined for the perovskite and post-perovskite polymorphs of Al$_2$O$_3$ can be seen in Figure 2, with calculated shear-wave splitting for selected propagation directions listed in Table 3. The compressional-wave velocities of both polymorphs show a regular decrease in magnitude at increased temperature. In contrast, the shear-wave velocities decrease in a much less uniform manner, in particular for the perovskite phases, where the degree of shear-wave splitting for a particular propagation direction varies with temperature. Similar behavior is exhibited by the perovskite and post-perovskite phases of MgSiO$_3$

Table 1. Calculated Elastic Moduli of Perovskite and Post-Perovskite Polymorphs of Al$_2$O$_3$ and MgSiO$_3$ (in GPa)

P/GPa	T/K	C_{11}	C_{22}	C_{33}	C_{12}	C_{13}	C_{23}	C_{44}	C_{55}	C_{66}	K	G
Perovskite Phase of Al$_2$O$_3$												
136	0	988	1329	978	511	482	509	267	259	317	685	285
136	4000	891	1120	804	530	352	388	188	236	209	571	227
Post-Perovskite Phase of Al$_2$O$_3$												
136	0	1344	1089	1122	437	421	580	260	144	404	714	281
136	4000	1155	884	963	409	441	532	249	51	291	637	185
Perovskite Phase of MgSiO$_3$[a]												
136	0	955	1239	1186	562	448	472	376	277	369	695	326
136	4000	857	1130	941	523	383	513	281	263	284	619	265
Post-Perovskite Phase of MgSiO$_3$[b]												
136	0	1332	995	1318	461	362	525	291	279	442	702	345
136	4000	1107	847	1131	429	318	441	251	221	361	604	285

[a]Taken from J. Wookey et al. (Efficacy of post-perovskite as an explanation for lowermost mantle seismic properties, submitted to *Nature*, 2005, hereinafter referred to as Wookey et al., submitted manuscript, 2005).
[b]Taken from *Stackhouse et al.* [2005].

Table 2. Calculated Cell Parameters of Perovskite and Post-Perovskite Polymorphs of Al$_2$O$_3$

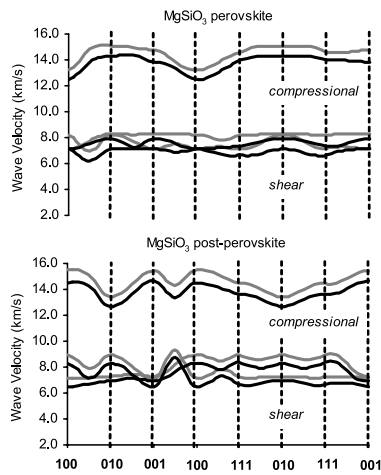| P/GPa	T/K	a/Å	b/Å	c/Å	V/Å^3	ρ/kg m^{-3}
Perovskite						
136	0	4.227	4.584	6.381	123.66	5477
136	4000	4.360	4.617	6.456	129.81	5131
Post-Perovskite						
136	0	2.455	8.053	6.142	121.43	5577
136	4000	2.506	8.175	6.235	127.71	5221

Figure 2. Variation of compressional and shear-wave velocities with propagation direction for the perovskite and post-perovskite polymorphs of MgSiO₃ at 136 GPa and 0 K – grey and 4000 K – black.

Figure 3. Variation of compressional and shear-wave velocities with propagation direction for the perovskite and post-perovskite polymorphs of Al₂O₃ at 136 GPa and 0 K – grey and 4000 K – black.

[*Stackhouse et al.*, 2005] shown in Figure 3. The most significant difference of the Al₂O₃ polymorphs, from those of MgSiO₃, is the much larger degree of shear-wave splitting exhibited by the perovskite phase, with a maximum over three times greater.

[11] Previous studies showed that, at 136 GPa and 4000 K, the pure end-member MgSiO₃ post-perovskite phase exhibits shear-wave splitting on the order of about twenty percent in the [100], [010] and [111] directions, while only five percent is seen in the [001] direction [*Stackhouse et al.*, 2005]. In the case of the pure end-member Al₂O₃ post-perovskite phase shear-wave splitting of approximately seventy, ten and thirty percent is seen in the [100], [010] and [111] directions and over sixty percent in the [001] direction. One could therefore speculate that a possible noticeable effect of incorporation of a few mole percent Al₂O₃ into the MgSiO₃ post-perovskite phase on observed shear-wave splitting would be an increase in the [100] and [001] directions. The potential geophysical implications of these results depend, however, on how the crystals would align themselves via lattice preferred orientation, which is proposed to develop by dislocation creep at the core-mantle boundary [*McNamara et al.*, 2001].

[12] Evidence exists for the core-mantle boundary being transversely isotropic in some regions [*Thomas and Kendall*, 2002]. It is therefore useful to determine the seismic anisotropy of transversely isotropic aggregates of the perovskite and post-perovskite polymorphs of pure end-
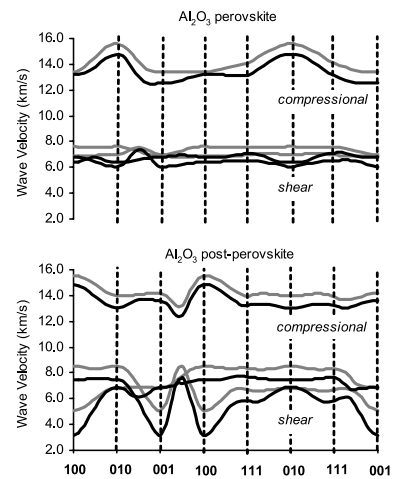
member Al₂O₃, listed in Table 4. It can be seen that transversely isotropic aggregates of the post-perovskite phase, with symmetry along [100] and [001] exhibit considerable shear-wave splitting, with the polarization $V_{SH} > V_{SV}$, as is generally seen for the last few hundred kilometers near the core-mantle boundary [*Panning and Romanowicz*, 2004]. In fact, the most obvious slip-plane, that parallel to the silicate layers, would produce a transversely isotropic aggregate with a symmetry axis along the [010] direction, which exhibits shear-wave splitting with the opposite polarization i.e., $V_{SV} > V_{SH}$. Note that for the analogous MgSiO₃ aggregate the observed polarization is produced [*Stackhouse et al.*, 2005]. The definitive slip system for the post-perovskite phase, however, is still unknown.

[13] The bulk seismic velocities of the perovskite and post-perovskite phases of both MgSiO₃ and Al₂O₃ are listed in Table 5. In the case of MgSiO₃ no significant difference is seen in compressional-wave velocity when going from perovskite to post-perovskite, while the shear-wave velocity increases by 3.1 percent and bulk sound velocity decreases by 2.0 percent. This is consistent with seismic observations at the base of the mantle, where the phase transition is expected to occur [*Sidorin et al.*, 1998; *Su and Dziewonski*, 1997]. In the case of Al₂O₃ again little difference is seen in the compressional-wave velocity when going from perovskite to post-perovskite, but the shear-wave velocity decreases by over 11.1 percent and the bulk sound velocity increases by a 4.6 percent, the opposite relation to seismic observations. If we assume simple linear mixing, our results

Table 3. Calculated Shear-Wave Splitting ((V_{S1} – V_{S2})/⟨V_S⟩)*100 for Perovskite and Post-Perovskite Polymorphs of Al₂O₃ in Various Propagation Directions[a]

P/GPa	T/K	100	010	001	110	111
Perovskite						
136	0	10.23	8.75	1.48	9.10	8.92
136	4000	5.98	4.98	10.96	4.80	8.84
Post-Perovskite						
136	0	48.4	23.6	24.7	32.3	22.8
136	4000	72.8	9.57	63.3	37.0	30.8

[a]Note that V_{S1} is taken to be the faster than V_{S2} in each case.

Table 4. Seismic Wave Velocity Anisotropy for Transversely Isotropic Aggregates of Perovskite and Post-Perovskite Polymorphs of Al₂O₃ With Symmetry Axis Along [100], [010] and [001] Directions[a]

	[001]	[010]	[100]
Perovskite (compressional)	10.61	−15.1	1.17
Perovskite (shear)	2.60	9.72	3.27
Post-perovskite (compressional)	2.63	2.59	−10.6
Post-perovskite (shear)	36.9	−22.1	13.4

[a]Note that a positive value infers that the horizontally polarized wave travels faster than that vertically polarized and vice versa.

Table 5. Compressional (V$_P$), Shear (V$_S$) and Bulk (V$_\Phi$) Isotropic Wave Velocities (in km s^{-1}) of Perovskite and Post-Perovskite Polymorphs of Al$_2$O$_3$ and MgSiO$_3$ at 136 GPa and 4000 K

	V_P	V_S	V_Φ
Perovskite phase of Al$_2$O$_3$	13.0	6.65	10.5
Post-perovskite phase of Al$_2$O$_3$	13.0	5.95	11.0
Perovskite phase of MgSiO$_3$[a]	13.7	7.14	10.9
Post-perovskite phase of MgSiO$_3$[b]	13.7	7.36	10.7

[a]Taken from Wookey et al. (submitted manuscript, 2005).
[b]Taken from *Stackhouse et al.* [2005].

imply that in the mantle incorporation of aluminum into MgSiO$_3$ reduces anti-correlation of bulk sound and shear-wave velocities and decreases the shear-wave velocity discontinuity from 3.1 to 2.6 percent.

[14] The incorporation of a few mole percent of Al$_2$O$_3$ into MgSiO$_3$ is predicted to have little effect on the perovskite to post-perovskite transition pressure. Small changes in the seismic properties of the post-perovskite phase are compatible with observations for the base of the mantle.

References

Akber-Knutson, S., and M. S. T. Bukowinski (2004), The energetics of aluminum solubility into MgSiO$_3$ perovskite at lower mantle conditions, *Earth Planet. Sci. Lett.*, *220*, 317–330.

Anderson, D. L. (1989), *Theory of the Earth*, 148 pp., Blackwell Sci., Malden, Mass.

Blöchl, P. R. (1994), Projector augmented-wave method, *Phys. Rev. B.*, *50*, 17,953–17,979.

Brodholt, J. P. (2000), Pressure-induced changes in the compression mechanism of aluminous perovskite in the Earth's mantle, *Nature*, *407*, 620–622.

Caracas, R., and R. C. Cohen (2005), Prediction of a new phase transition in Al$_2$O$_3$ at high pressures, *Geophys. Res. Lett.*, *32*, L06303, doi:10.1029/2004GL022204.

Iitaka, T., K. Hirose, K. Kawamura, and M. Murakami (2004), The elasticity of the MgSiO$_3$ post-perovskite phase in the Earth's lowermost mantle, *Nature*, *430*, 442–445.

Irifune, T. (1994), Absence of an aluminous phase in the upper part of the Earth's lower mantle, *Nature*, *370*, 131–133.

Kendall, J.-M., and P. G. Silver (1998), Investigating causes of D″ anisotropy, in *The Core-Mantle Boundary Region*, *Geodyn. Ser.*, vol. 28, edited by M. Gurnis et al., pp. 97–118, AGU, Washington, D. C.

Kresse, G., and J. Furthmüller (1996a), Efficient interative schemes for ab initio total-energy calculations using a plane-wave basis set, *Phys. Rev. B*, *54*, 11,169–11,186.

Kresse, G., and J. Furthmüller (1996b), Efficiency of ab initio total energy calculations for metals and semiconductors using a plane-wave basis set, *Comput. Mater. Sci.*, *6*, 15–50.

Kresse, G., and D. Joubert (1999), From ultrasoft pseudopotentials to the projector augmented-wave method, *Phys. Rev. B*, *59*, 1758–1775.

Mao, W. L., G. Shen, V. B. Prakapenka, Y. Meng, A. J. Campbell, D. L. Heinz, J. Shu, R. J. Hemley, and H.-K. Mao (2004), Ferromagnesian

post-perovskite silicates in the D″ layer, *Proc. Natl. Acad. Sci. U. S. A.*, *101*, 15,867–15,869.

McNamara, A. K., S.-H. Karato, and P. E. van Keken (2001), Localization of dislocation creep in the lower mantle: Implications for the origin of seismic anisotropy, *Earth Planet. Sci. Lett.*, *191*, 85–99.

Monkhorst, H. J., and J. D. Pack (1976), Special points for Brillouin-zone integrations, *Phys. Rev. B*, *13*, 5188–5192.

Murakami, M., K. Hirose, K. Kawamura, N. Sata, and Y. Ohishi (2004), Post-perovskite phase transition in MgSiO$_3$, *Science*, *304*, 855–858.

Musgrave, M. J. P. (1970), *Crystal Acoustics*, Holden-Day, Boca Raton, Fla.

Oganov, A. R., J. P. Brodholt, and G. D. Price (2001), The elastic constants of MgSiO$_3$ perovskite at pressures and temperatures of the Earth's mantle, *Nature*, *411*, 934–937.

Oganov, A. R., and S. Ono (2004), Theoretical and experimental evidence for a post-perovskite phase of MgSiO$_3$ in Earth's D″ layer, *Nature*, *430*, 445–448.

Panning, M., and B. Romanowicz (2004), Inferences on flow at the base of Earth's mantle based on seismic anisotropy, *Science*, *303*, 351–353.

Perdew, J. P., J. A. Chevary, S. H. Vosko, K. A. Jackson, M. R. Pederson, D. J. Singh, and C. Fiolhais (1992), Atoms, molecules, solids, and surfaces—Applications of the generalized gradient approximation for exchange and correlation, *Phys. Rev. B*, *46*, 6671–6687.

Shim, S. H., T. S. Duffy, R. Jeanloz, and G. Shen (2004), Stability and crystal structure of MgSiO$_3$ perovskite to the core-mantle boundary, *Geophys. Res. Lett.*, *31*, L10603, doi:10.1029/2004GL019639.

Sidorin, I., M. Gurnis, D. V. Helmberger, and X. Ding (1998), Interpreting D″ seismic structure using synthetic waveforms computed from dynamic models, *Earth Planet. Sci. Lett.*, *163*, 31–41.

Sidorin, I., M. Gurnis, and D. V. Helmberger (1999), Evidence for a ubiquitous seismic discontinuity at the base of the mantle, *Science*, *286*, 1326–1331.

Stackhouse, S., J. P. Brodholt, J. Wookey, J.-M. Kendall, and G. D. Price (2005), The effect of temperature on the seismic anisotropy of the perovskite and post-perovskite polymorphs of MgSiO$_3$, *Earth Planet. Sci. Lett.*, *230*, 1–10.

Su, W.-J., and A. M. Dziewonski (1997), Simultaneous inversion for 3-D variations in shear and bulk velocity in the mantle, *Phys. Earth Planet. Inter.*, *100*, 135–156.

Thomas, C., and J.-M. Kendall (2002), The lowermost mantle beneath northern Asia—II. Evidence for lower-mantle anisotropy, *Geophys. J. Int.*, *151*, 296–308.

Tsuchiya, T., J. Tsuchiya, K. Umemoto, and R. M. Wentzcovitch (2004a), Phase transition in MgSiO$_3$ perovskite in the earth's lower mantle, *Earth Planet. Sci. Lett.*, *224*, 241–248.

Tsuchiya, T., J. Tsuchiya, K. Umemoto, and R. M. Wentzcovitch (2004b), Elasticity of post-perovskite MgSiO$_3$, *Geophys. Res. Lett.*, *31*, L14603, doi:10.1029/2004GL020278.

Wang, Y., and J. P. Perdew (1991), Correlation hole of the spin-polarized electron-gas, with exact small-wave-vector and high density scaling, *Phys. Rev. B*, *44*, 13,298–13,307.

Wentzcovitch, R. M., B. B. Karki, S. Karoto, and C. R. S. Da Silva (1998), High pressure elastic anisotropy of MgSiO$_3$ perovskite and geophysical implications, *Earth Planet. Sci. Lett.*, *164*, 371–378.

Wood, B. J., and D. C. Rubie (1996), The effect of alumina on phase transformations at the 600-kilometer discontinuity from Fe-Mg partitioning experiments, *Science*, *273*, 1522–1524.

Yamamoto, T., D. A. Yuen, and T. Ebisuzaki (2003), Substitution mechanism of Al ions in MgSiO$_3$ perovskite under high pressure conditions from first-principles calculations, *Earth Planet. Sci. Lett.*, *206*, 617–625.

————————————

J. P. Brodholt, G. D. Price, and S. Stackhouse, Department of Earth Sciences, University College London, Gower Street, London, WC1E 6BT, UK. (s.stackhouse@ucl.ac.uk)